

A Toy Model for Low Energy Nuclear Fusion

K. Ramkumar^{*1}, Harishyam Kumar^{†1}, and Pankaj Jain^{‡2}

¹Department of Physics, Indian Institute of Technology, Kanpur

²Department of Space Science & Astronomy, Indian Institute of Technology,
Kanpur

June 2022

Abstract

We study the fusion of a proton with a nucleus with the emission of two photons at low incident energy of the order of eV or smaller. We use a step model for the repulsive potential between proton and the nuclei. We consider the reaction both in free space and inside a medium. We make a simple model for the medium by assuming a hard wall potential beyond a certain length scale. This essentially leads to discretization of the energy spectrum which is expected inside a medium and is seen both for a crystalline lattice structure and for amorphous materials. We use second order perturbation theory to compute the transition rate. We find that the rate in free space is very small. However in medium, the rate may be substantial. Hence, we conclude that nuclear fusion reactions may take place at low energies at observable rates.

1 Introduction

The nuclear fusion processes are expected to be strongly suppressed at low energies [1]. There have been experimental claims that such processes may be occurring at observable rates in a medium, see for example [2, 3, 4, 5]. However, despite considerable effort [6, 7, 8, 9, 10], so far there does not exist any reliable theoretical model of how this can happen. A useful review of the shortcomings of a wide range of theoretical proposals is given in [11].

In [12, 13], the authors have explored the possibility that low energy fusion may arise at second order in perturbation theory. A similar idea has also been proposed in [14]. At this order we need to sum over all the intermediate state energies and hence the Coulomb barrier may not be very prohibitive. The process considered in [12, 13] involves two interactions or vertices and involves emission of two photons, one at each vertex. The process may be expressed as,

$${}^1H + {}^AX \rightarrow {}^{A+1}Y + \gamma(\omega_1) + \gamma(\omega_2) \quad (1)$$

where 1H denotes the Hydrogen, AX a nucleus with atomic number Z and mass number A and ${}^{A+1}Y$ a nucleus with atomic number $Z + 1$ and mass number $A + 1$. The emitted photons have frequencies ω_1 and ω_2 . This may be compared to the related first order process,

$${}^1H + {}^AX \rightarrow {}^{A+1}Y + \gamma(\omega) \quad (2)$$

*ramkumar@iitk.ac.in

†hari@iitk.ac.in

‡pkjain@iitk.ac.in

which is the standard fusion process with emission of a photon.

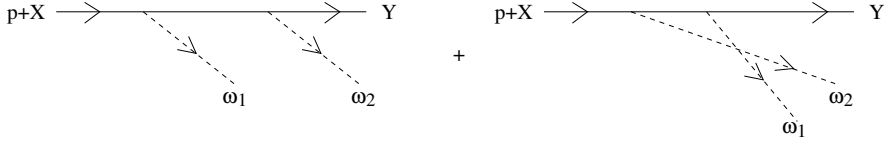


Figure 1: The two amplitudes contributing to the nuclear fusion process with two photon emission.

At second order in perturbation theory, the two photon emission process, Eq. 1 gets contributions from two amplitudes which are shown in Fig. 1. At the first interaction or vertex the proton or the X nucleus emits a photon forming an intermediate state consisting of a proton and X. We work in the center of mass and relative coordinates and only the relative coordinates are relevant [12, 13]. In the intermediate state we need to sum over states of all energy, without imposing energy conservation at either of the two vertices. Of course, the total energy has to be conserved. At the second vertex, the proton gets captured by the nucleus X with emission of another photon. The process, therefore, involves two matrix elements one for each vertex. In earlier papers [12, 13], the authors refer to the first matrix element as the molecular matrix element since it gets dominant contributions from distances of order 1 atomic unit, while the second matrix element gets contributions dominantly from nuclear distances and is called nuclear matrix element.

The important point is that we need to sum over intermediate states of all energies. Since the initial state has very small energy E_i and momentum, the molecular matrix element is appreciable only when the energy of the intermediate state E_n is such that the corresponding momentum \vec{P}_n closely balances the photon momentum \vec{P}_γ . One might expect that the dominant contribution to the entire amplitude would come from $\vec{P}_n \approx P_\gamma$ with the corresponding energy $E_n \gg E_i$, thereby leading to a rather large amplitude. However, explicit calculations in [12, 13] show that this fails. The problem is that here we are dealing with particles in a potential and hence the energy eigenstates are not eigenstates of momentum. Due to this the molecular matrix element does not select a unique value of \vec{P}_n and a large range of values of $P_n = |\vec{P}_n|$ contribute. Explicit calculations show that these cancel among one another leading to a very small amplitude.

In [12, 13], the authors suggested several possibilities which might evade the acute cancellation described above. One suggestion was that in a medium, the energy eigenvalues are discrete and do not form a continuous set as in free space. In such a case, the cancellation may not be complete and we may get a substantial contribution. We test this possibility in detail in the present paper, assuming a step function potential for the tunneling barrier. This captures the essential details of the process while facilitating mathematical calculations. Calculation with Coulomb is postponed to future work. Another suggestion in [12, 13] was the presence of a resonant nuclear state at energy $E_R \gg E_i$. In this case, the dominant contribution will arise from energies very close to E_R which may not cancel out. We briefly comment on this possibility also in the present paper.

We also point out that in our paper we have confined ourselves to one process in order to demonstrate that low energy nuclear reactions are possible. There may be other processes which may not involve emission of photons and might proceed at higher rates. This needs to be studied in detail in future. While demonstrating the theoretical possibility of such reactions to occur at observable rates, our work paves the way for study of other related processes.

2 Potential Model and Wave functions

In this section, we give the potential model used for the calculations and the corresponding energy eigenstates. As mentioned in the Introduction we use a step function for the potential barrier instead of the standard Coulomb potential. This has the advantage that the wave functions can be computed analytically.

We assume a spherically symmetric potential which can be written as,

$$V(r) = \begin{cases} -V_0 & r < L_n \\ V_1 & L_n \leq r \leq L_b \\ 0 & L_c \geq r > L_b \\ V_2 & r > L_c \end{cases} \quad (3)$$

where V_0 is the nuclear potential, V_1 represents our model for the tunneling barrier and we shall take V_2 to be infinitely large. The potential is shown schematically in Fig. 2. A possible set of parameters are $V_0 = 50$ MeV, $V_1 = 100$ in atomic units (Hartree), the nuclear length scale $L_n = 0.9566 \times 10^{-4}$ atomic units (a.u.) and the barrier length scale $L_b = 0.1$ a.u.. We point out that 1 Hartree is approximately 27.2 eV and the atomic unit for length is Bohr radius. The cutoff length scale L_c is not shown in Fig. 2. We assume that the potential V_2 beyond this point is infinitely large. Hence all the wave functions are set to zero at this radius.

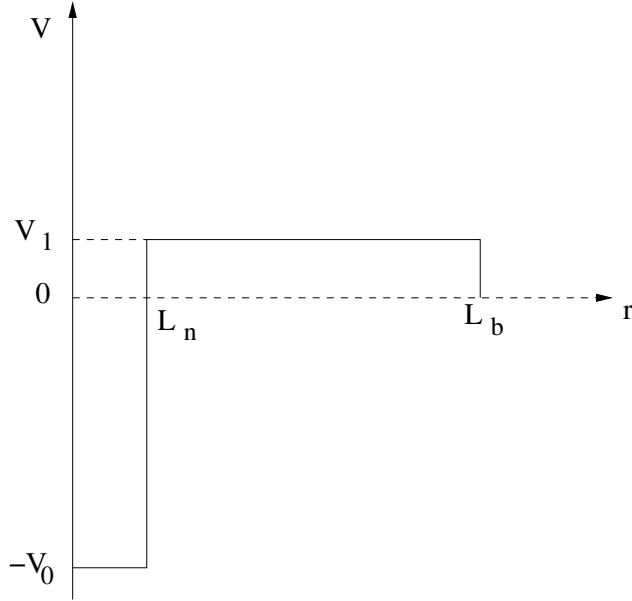


Figure 2: Schematic illustration of the model potential.

The potential model represents a mathematically well defined quantum system. It also approximately describes a physical situation in which we have a small spherically symmetric cavity in a solid material composed of element with large atomic mass. In the cavity we assume presence of a gas composed of Hydrogen and a relatively heavier element X. We are considering fusion of Hydrogen with X. The effect of solid matter is to simply discretize the energy eigenvalues of

the H–X system. Each lattice site of the solid matter presents a very high potential barrier to H–X system. We assume that this barrier height $V_2 \gg V_1$ and, for simplicity, we approximate it as infinity. If this forms a regular lattice, we expect the formation of bands as in the case of an electronic system [15]. Alternatively if there is sufficient disorder in the system, we may only have a few localized states, analogous to Anderson localization [16, 17]. Here we have simply modelled this system by assuming that the overall effect of the lattice sites is to present an almost infinite potential barrier once we go to sufficiently large radius from the cavity. This will lead to discretization of the energy levels which is qualitatively similar to the band structure we expect for a crystalline lattice, in the sense that both lead to non-continuous quantum states.

The potential given in Eq. 3 can be solved analytically. We are interested in the two particle wave function. The center of mass wave function is not relevant to our analysis [12, 13] and we focus on the relative coordinate \vec{r} . For $l = 0$ the wave function depends only on $r = |\vec{r}|$ and can be expressed as,

$$\psi(r) = Y_0^0 \frac{U(r)}{r}. \quad (4)$$

where $Y_0^0 = 1/\sqrt{4\pi}$. For energy eigenvalue $E < V_1$, we obtain,

$$U(r) = \frac{1}{N'_L} \sin(K_1 r) \quad \text{for } r < L_n \quad (5a)$$

$$U(r) = \frac{1}{N'_L} [B_L e^{-K_2 r} + C_L e^{K_2 r}] \quad \text{for } L_n \leq r \leq L_b \quad (5b)$$

$$U(r) = \frac{1}{N'_L} [D_L \sin(K r) + F_L \cos(K r)] \quad \text{for } L_b < r \leq L_c \quad (5c)$$

$$U(r) = 0 \quad \text{for } r > L_c \quad (5d)$$

where,

$$K = \sqrt{\frac{2mE}{\hbar^2}}, \quad K_1 = \sqrt{\frac{2m(E - V_0)}{\hbar^2}}, \quad K_2 = \sqrt{\frac{2m(V_1 - E)}{\hbar^2}}, \quad (6)$$

$$N'_L = K N_L, \quad N_L = \sqrt{D_L^2 + F_L^2}, \quad (7)$$

$$B_L = \frac{b}{2 K_2 e^{-K_2 L_n}}, \quad C_L = \frac{c}{2 K_2 e^{K_2 L_n}}, \quad (8)$$

$$b = -K_1 \cos(K_1 L_n) + K_2 \sin(K_1 L_n) \quad (9)$$

$$c = K_1 \cos(K_1 L_n) + K_2 \sin(K_1 L_n) \quad (10)$$

and

$$D_L = (B_L e^{-K_2 L_b} + C_L e^{K_2 L_b}) \sin(K L_b) - \frac{K_2}{K} (B_L e^{-K_2 L_b} - C_L e^{K_2 L_b}) \cos(K L_b) \quad (11a)$$

$$F_L = (B_L e^{-K_2 L_b} + C_L e^{K_2 L_b}) \cos(K L_b) + \frac{K_2}{K} (B_L e^{-K_2 L_b} - C_L e^{K_2 L_b}) \sin(K L_b) \quad (11b)$$

Furthermore we have

$$D_L \sin(K L_c) + F_L \cos(K L_c) = 0 \quad (12)$$

Due to the boundary condition at L_c we get discrete energy eigenvalues and each eigenfunction is normalized to unity.

For $E \geq V_1$, the eigenfunctions for $r < L_n$ and $r > L_b$ have the same form as for $E < V_1$ with N'_L , D_L and F_L replaced by N'_H , D_H and F_H respectively. In the region $L_n \leq r \leq L_b$, it takes the form,

$$U(r) = \frac{1}{N'_L} \left[B_H \sin(\tilde{K}_2 r) + C_H \cos(\tilde{K}_2 r) \right] \quad \text{for } L_n \leq r \leq L_b \quad (13)$$

with

$$\tilde{K}_2 = \sqrt{\frac{2m(E - V_1)}{\hbar^2}} \quad (14)$$

The coefficients are given by

$$\begin{aligned} B_H &= \frac{K_1}{\tilde{K}_2} \cos(K_1 L_n) \cos(\tilde{K}_2 L_n) + \sin(K_1 L_n) \sin(\tilde{K}_2 L_n) \\ C_H &= -\frac{K_1}{\tilde{K}_2} \cos(K_1 L_n) \sin(\tilde{K}_2 L_n) + \sin(K_1 L_n) \cos(\tilde{K}_2 L_n) \\ D_H &= \left(B_H \sin(\tilde{K}_2 L_b) + C_H \cos(\tilde{K}_2 L_b) \right) \sin(K L_b) \\ &\quad + \frac{\tilde{K}_2}{K} \left(B_H \cos(\tilde{K}_2 L_b) - C_H \sin(\tilde{K}_2 L_b) \right) \cos(K L_b) \\ F_H &= \left(B_H \sin(\tilde{K}_2 L_b) + C_H \cos(\tilde{K}_2 L_b) \right) \cos(K L_b) \\ &\quad - \frac{\tilde{K}_2}{K} \left(B_H \cos(\tilde{K}_2 L_b) - C_H \sin(\tilde{K}_2 L_b) \right) \sin(K L_b) \end{aligned} \quad (15)$$

The final state wave function is taken to be $l = 1$. In our calculation we take a particular initial and final state. This is sufficient to determine whether fusion is facilitated by the second order mechanism. The detailed angular and spin dependence of the wave functions is given below.

In our analysis we shall assume that the initial state energy E_i is very small, of order 0.1 eV. For such energy the standard leading order process Eq. 2 is very strongly suppressed since the initial state wave function is negligible at small nuclear distances. The second order process Eq. 1, however, gets contributions from all energy eigenvalues in the intermediate state. For large energy, the corresponding eigenstates may take large values at small distances. Hence it is possible that the corresponding amplitude may be large.

3 Reaction Rate at First Order

In this section we compute the cross section for the leading order process given in Eq. 2. This is useful for comparison with the second order resonant process, discussed in the next section. We assume that the nucleus ${}^A X$ has spin 0 and $l = 0$ in the ground state. We consider the transition from initial state composed of ${}^1 H$ and ${}^A X$ with $l = 0$ to the final state ${}^{A+1} Y$ with $l = 1$. The spin wave function of proton does not play any role in this transition. For the chosen potential parameters, the final state has energy eigenvalue $E_f = -13.5$ MeV and the corresponding wave function is shown in Fig. 3.

We may write the Hamiltonian as,

$$H = H_0 + H_I \quad (16)$$

where H_0 is the unperturbed Hamiltonian and H_I the electromagnetic perturbation. We can write H_0 as,

$$H_0 = \mathcal{K}_1 + \mathcal{K}_2 + V(r) \quad (17)$$

where \mathcal{K}_1 and \mathcal{K}_2 are the kinetic energies of the 1H and the AX nucleus respectively and $V(r)$ the potential given in Eq. 3. Here we focus on the relative motion relevant for the fusion process. The relative coordinate is denoted by \vec{r} , such that, $\vec{r} = \vec{r}_2 - \vec{r}_1$, where \vec{r}_1 and \vec{r}_2 are the coordinates of the 1H and AX nucleus. The potential is assumed to be spherically symmetric and depends only on the magnitude $r = |\vec{r}|$. We express the kinetic energies in terms of the center of mass and relative momenta and focus on the relative momentum.

The perturbation H_I can be expressed as [18, 19]

$$H_I(t) = -\frac{Z_1 e}{cm_1} \vec{A}(\vec{r}_1, t) \cdot \vec{p}_1 - \frac{Z_2 e}{cm_2} \vec{A}(\vec{r}_2, t) \cdot \vec{p}_2 + \frac{e\hbar g_p}{2m_1 c} \vec{\sigma} \cdot \vec{B} + \dots \quad (18)$$

where Z_1 , m_1 and \vec{p}_1 are the atomic number, mass and momentum of the 1H . The corresponding quantities for AX are Z_2 , m_2 and \vec{p}_2 . Furthermore, σ_i are the Pauli matrices, g_p the proton g factor, \vec{A} is the vector potential,

$$\vec{A}(\vec{r}, t) = \frac{1}{\sqrt{\Omega}} \sum_{\vec{k}} \sum_{\beta} c \sqrt{\frac{\hbar}{2\omega}} \left[a_{\vec{k},\beta}(t) \vec{\epsilon}_{\beta} e^{i\vec{k}\cdot\vec{r}} + a_{\vec{k},\beta}^{\dagger}(t) \vec{\epsilon}_{\beta}^* e^{-i\vec{k}\cdot\vec{r}} \right] \quad (19)$$

and $\vec{B} = \vec{\nabla} \times \vec{A}$ is the magnetic field. The vector potential is expressed in terms of the photon polarization vector ϵ_{β} , the wave vector \vec{k} the frequency ω and the total volume Ω .

We next compute the rate for $l = 0$ to $l = 1$ transition at first order in perturbation theory. We consider a particular process in which the initial state proton is in spin up state. The final state is taken to be $j = 3/2$ and $j_z = 3/2$. The corresponding rate is given by,

$$\Gamma_1 = \frac{4\alpha\xi^2 E_p^3}{3\hbar^3 c^2} |\langle \psi_f | r | \psi_i \rangle|^2 \quad (20)$$

where E_p is the energy of the photon emitted as given by the conservation of energy,

$$E_p = E_f - E_i$$

We evaluate the reaction rate by setting the cutoff length scale $L_c = 10$ atomic units. For such a length scale we find an eigenstate with energy equal to $E_i = 0.0903$ eV. For the model potential we are considering, the reaction rate for this state is found to be 10^{-44} per second.

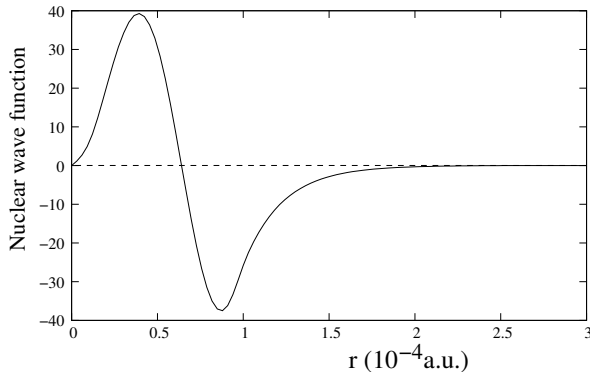


Figure 3: The final state nuclear wave function ($l = 1$) corresponding to energy eigenvalue -13.5 MeV.

3.1 Transition Rate at Second Order

In this section we compute the transition rate for the process given in Eq. 1 which goes by emission of two photons. This gets dominant contribution at second order in perturbation theory. The transition amplitude in this order is given by,

$$\begin{aligned} \langle f | T(t_0, t) | i \rangle &= \left(\frac{-i}{\hbar} \right)^2 \sum_n \int_{t_0}^t dt' \langle f | e^{i H_0 t' / \hbar} H_I(t') e^{-i H_0 t' / \hbar} | n \rangle \\ &\times \int_{t_0}^{t'} dt'' \langle n | e^{i H_0 t'' / \hbar} H_I(t'') e^{-i H_0 t'' / \hbar} | i \rangle \end{aligned} \quad (21)$$

where H_I is given by Eq. 18. As mentioned above, we take the initial state to be $l = 0$, spin $1/2$ with $S_z = -1/2$, corresponding to the spin of the proton. For the first transition from initial to intermediate state we consider contribution from the magnetic term in Eq. 18. This transition does not change l but flips the spin of the proton. The transition from intermediate to final state is taken to be $l = 0$ to $l = 1$ with no change in spin. This gets dominant contribution from first two terms on the right hand side in Eq. 18. Hence the total transition is $l = 0$ to $l = 1$ along with a flip of the proton spin. We take the final state to be $j = 3/2$ with $j_z = 3/2$.

We point out that there is another contribution to this transition with the first two terms on right hand side of Eq. 18 contributing at the first interaction and the last term contributing at the second interaction. This will lead to a transition $l = 0$ to $l = 1$ to $l = 1$ and will involve an $l = 1$ intermediate state. This contribution involves the effective momentum of the initial state wave function k_i and is suppressed in comparison to the amplitude described in the previous paragraph. Furthermore the fusion process takes place through an $l = 1$ state which is suppressed compared to that for $l = 0$. Finally the intermediate to final state process involves a magnetic transition which is known to be suppressed compared to an electric transition. Hence we expect this amplitude to be small and do not consider it further.

The matrix element at the first vertex is given by,

$$\langle n | H_I(t) | i \rangle = \frac{i e \hbar g_p k_1}{2m_1 \sqrt{\Omega}} \sqrt{\frac{\hbar}{2\omega_1}} \langle n | \vec{\sigma} \cdot (\hat{k}_1 \times \hat{\epsilon}^*) a^\dagger e^{-i \vec{k}_1 \cdot \vec{r} + i\omega_1 t} | i \rangle \quad (22)$$

There is one more term in this proportional to $1/m_2$ which is much smaller in the limit $m_2 \gg m_1$ and hence has been neglected [12]. Furthermore the exponent $\vec{k}_1 \cdot \vec{r}$ has a multiplicative factor

$m_2/(m_1 + m_2)$, which has been approximated as unity in the limit $m_2 \gg m_1$. Let us express the unit vector \hat{k}_1 as,

$$\hat{k}_1 = \cos \theta_1 \hat{z} + \sin \theta_1 [\cos \phi_1 \hat{x} + \sin \phi_1 \hat{y}] \quad (23)$$

We take the two photon polarization vectors to be

$$\begin{aligned} \hat{\epsilon}_1 &= -\sin \theta_1 \hat{z} + \cos \theta_1 [\cos \phi_1 \hat{x} + \sin \phi_1 \hat{y}] \\ \hat{\epsilon}_2 &= -\sin \phi_1 \hat{x} + \cos \phi_1 \hat{y} \end{aligned} \quad (24)$$

We consider the contribution only from $\hat{\epsilon}_1$. This is sufficient for our purpose since the contribution from $\hat{\epsilon}_2$ will add incoherently and can only change the result by a factor of order unity. In any case the other polarization does not contribute to the particular transition being considered. Using $\hat{k}_1 \times \hat{\epsilon}_1 = \hat{\epsilon}_2$, we obtain,

$$\vec{s} \cdot (\hat{k}_1 \times \hat{\epsilon}_1) = \cos \phi_1 s_y - \sin \phi_1 s_x \quad (25)$$

where $\vec{s} = \vec{\sigma}/2$.

The matrix element in the right hand side can now be written as,

$$\langle n | \vec{\sigma} \cdot (\hat{k}_1 \times \hat{\epsilon}_1) a^\dagger e^{-i \vec{k}_1 \cdot \vec{r} + i \omega_1 t} | i \rangle = \langle n | e^{-i \vec{k}_1 \cdot \vec{r} + i \omega_1 t} | i \rangle (-i \cos \phi_1 - \sin \phi_1) \quad (26)$$

where the spin part has been evaluated. In the spatial part of the matrix element, only the $l = 0$ term of the photon wave function contribute. Hence using plane wave expansion and doing the angular integral, we obtain,

$$\langle n | e^{-i \vec{k}_1 \cdot \vec{r} + i \omega_1 t} | i \rangle = e^{i \omega_1 t} \int dr U_n^* \frac{\sin(k_1 r)}{k_1 r} U_i \quad (27)$$

In this evaluation we have assumed that the photon with frequency ω_1 is emitted at the first vertex. As shown in Fig. 1, there are two contributions and either of the photons can be emitted at the first vertex. However, for the range of parameters considered, the second contribution corresponding to photon of frequency ω_2 emitted at the first vertex turns out to be much smaller. This is because of our choice of k_1 and k_2 values and is discussed later in section 4.

We next consider the matrix element from intermediate to final state. The emitted photon has wave vector \vec{k}_2 and frequency ω_2 . We denote the polar coordinates of the unit vector \hat{k}_2 by θ_2 and ϕ_2 . The polarization vectors are denoted by $\vec{\epsilon}'_1$ and $\vec{\epsilon}'_2$. These three unit vectors are given by Eqs. 23 and 24 with (θ_1, ϕ_1) replaced by (θ_2, ϕ_2) . We consider the nuclear final state with $j = 3/2$ and $j_z = 3/2$. The other states will add incoherently and including them will only produce a change of order unity. Hence, we ignore them here to focus on the main result. Furthermore we take the polarization vector of the photon produced at this vertex to be $\vec{\epsilon}'_2$. The matrix element evaluates to

$$\begin{aligned} \langle f | H_I(t) | n \rangle &= -e^{i \omega_2 t} i e \sqrt{\frac{1}{2 \Omega \omega_2 \hbar}} (E_f - E_n) \langle f | \vec{\epsilon}'_2 \cdot \vec{r} | n \rangle \\ &= -e^{i \omega_2 t} i e \sqrt{\frac{1}{12 \Omega \omega_2 \hbar}} (E_f - E_n) (\sin \phi_2 + i \cos \phi_2) \int dr U_f^* r U_n \end{aligned} \quad (28)$$

The reaction rate can be expressed as:

$$\frac{dP}{dt} = \frac{1}{\Delta T} \int dE_1 dE_2 \rho_1 \rho_2 |\langle f | T(t_0, t) | i \rangle|^2 \quad (29)$$

where $E_1 = \hbar\omega_1$, $E_2 = \hbar\omega_2$ and ρ_1 is the photon density of state factor, given by,

$$\rho_1 = \frac{\Omega\omega_1^2}{(2\pi)^3} \frac{d\phi_1 d\cos\theta_1}{\hbar c^3} \quad (30)$$

along with a corresponding formula for ρ_2 . This leads to the following formula for the reaction rate

$$\frac{dP}{dt} = \frac{\alpha^2 g_p^2}{12\pi\hbar^3 c^6 m_p^2} \int dE_1 E_1^3 E_2 |I|^2 \quad (31)$$

$$I = \sum_n I_1 I_2 \frac{E_f - E_n}{E_n - E_i + E_1} \quad (32)$$

$$I_1 = \int dr U_n^* \frac{\sin(k_1 r)}{k_1 r} U_i \quad (33)$$

$$I_2 = \int dr' U_f^* r' U_n \quad (34)$$

where k_1 is the photon wave number. In Eq. 32, the sum over intermediate states runs over all the energy values from zero till infinity. We next turn to the calculation of the integrals I_1 , I_2 and the sum over energies. We point out that it is the sum over energies which led to the acute cancellation observed in [12, 13].

3.2 Computational Details

In this section we provide some details of the computation of the molecular matrix element, i.e. the integral I_1 , given in Eq. 33. Both the wave functions U_1 and U_n correspond to $l = 0$. For $r < L_b$ the wave function U_i decays very sharply. Hence the dominant contribution is obtained from $L_c > r > L_b$, although in our calculation we include contribution from all regions. The wave functions in the region $L_c > r > L_b$ can be expressed as,

$$U_n = \frac{1}{K_n N_n} [D_n \sin(K_n r) + F_n \cos(K_n r)] \quad (35)$$

$$U_i = \frac{1}{K_i N_i} [D_i \sin(K_i r) + F_i \cos(K_i r)] \quad (36)$$

Using these equations and simplifying I_1 we get a sum of 4 sine terms and 4 cosine terms, given below,

$$\begin{aligned} T_1 &= \sin((k_1 + K_n - K_i)r) [D_n D_i + F_n F_i] \\ T_2 &= \sin((k_1 - K_n + K_i)r) [D_n D_i + F_n F_i] \\ T_3 &= \sin((k_1 + K_n + K_i)r) [F_n F_i - D_n D_i] \\ T_4 &= \sin((k_1 - K_n - K_i)r) [F_n F_i - D_n D_i] \\ T_5 &= -\cos((k_1 + K_n - K_i)r) [D_n F_i - F_n D_i] \\ T_6 &= -\cos((k_1 - K_n + K_i)r) [F_n D_i - D_n F_i] \\ T_7 &= \cos((k_1 + K_n + K_i)r) [-F_n D_i - D_n F_i] \\ T_8 &= \cos((k_1 - K_n - K_i)r) [F_n D_i + D_n F_i] \end{aligned} \quad (37)$$

each with a pre-factor,

$$\frac{1}{4N_i K_i} \frac{1}{N_n K_n} \frac{1}{k_1 r}$$

For small K_i the dominant contribution comes from the kinematic region $K_n \approx k_1$ due to terms which involve $K_n - k_1$. The sum of these two wave numbers is very large and leads to negligible values of I_1 .

The integrals are facilitated by the following formulas,

$$\int_{L_b}^{L_c} \frac{\sin(\mathcal{K} r)}{r} dr = [\text{Si}(|\mathcal{K}| L_c) - \text{Si}(|\mathcal{K}| L_b)] \text{sgn}(\mathcal{K}) \quad (38)$$

where

$$\text{Si}(x) = \int_0^x dt \frac{\sin t}{t} \quad (39)$$

Similarly the cosine integral gives,

$$\int_{L_b}^{L_c} \frac{\cos(\mathcal{K} r)}{r} dr = \text{Ci}(|\mathcal{K}| L_c) - \text{Ci}(|\mathcal{K}| L_b) \quad (40)$$

where $\text{Ci}(x)$ can be expressed as,

$$\text{Ci}(x) = \gamma + \ln x - \int_0^x \frac{1 - \cos t}{t} dt \quad (41)$$

We similarly compute the integral in the region $r < L_b$.

We next consider the integral I_2 which appears in the nuclear matrix element. This integral gets dominant contribution from very small values of r . It shows a very mild dependence on intermediate state energy eigenvalue E_n for $E_n < V_1$, except for the factor N_n in the denominator. This essentially corresponds to a barrier penetration factor and shows an increase with E_n . For $E_n \gg V_1$, I_2 starts to oscillate with E_n .

4 Results

We first consider the case $L_c = \infty$. In this case the potential V_2 plays no role and we obtain a continuous energy spectrum. We take the initial energy eigenvalue E_i to be equal to 0.1 eV. As found earlier [12, 13] the amplitude becomes large in the regime when $K_n \approx k_1$. However adding over all intermediate eigenstates leads to a very small result. The precise value is difficult to compute numerically but we find a cancellation up to six significant digits. This suggests that the rate in free space is very small. This result is in agreement with what was found in [12, 13]. We also test the possibility that rate may be enhanced if the photon wave number k_1 is set equal to the wave number K_n of an intermediate state which corresponds to a nuclear resonance. We find that even in this case the rate turns to be very small due to a delicate cancellation.

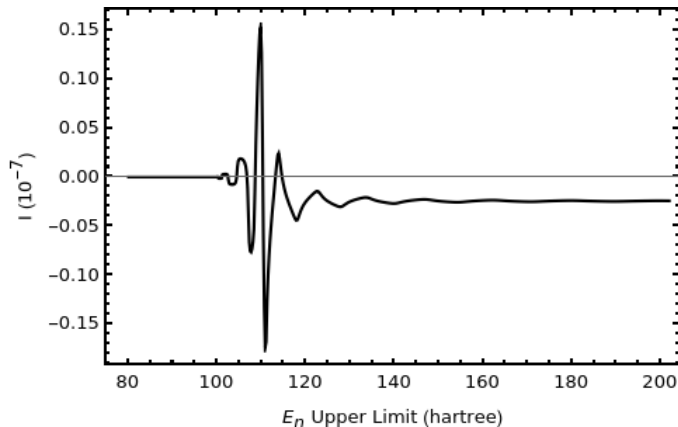


Figure 4: The amplitude I (Eq. 32) as a function of the upper limit on the energy E_n of the intermediate state. Here the photon wave number has been set equal to 635 atomic units and $L_c = 10$.

We next compute the rate for a finite value of L_c which would be applicable in a medium. We first take a relatively small value of $L_c = 10$ in atomic units. This will lead to a relatively large separation in energy among different states. We may compare this value with the level spacing in the case of Kronig-Penney model which is a one dimensional periodic potential. We find that the level spacing in this case is determined by the width of the potential wells [18]. This in our case would represent the distance between the lattice sites in the medium and hence would be of order a few atomic units. Hence the choice $L_c = 10$ is not unphysical. For this value we find an energy eigenvalue at $E_i = 0.0903$ eV which we take to be the initial state energy. We take the photon wavenumber k_1 close to 600 atomic units. In this case the amplitude is quite large. In Fig. 4 we show the amplitude I , defined in Eq. 32 as a function of the upper limit on the intermediate state energy E_n for photon wave number $k_1 = 635$ atomic units. We see that the amplitude settles to a finite value as $E_n \rightarrow \infty$. The dependence of rate on the photon wavenumber is shown in Fig. 5. We find a rate of the order of 10^{-18} per second for the photon wave number close to 600 atomic units. The rate in this case is much larger than that found for the first order transition. If we set the chosen photon wave number equal to intermediate state wave number K_n , the corresponding intermediate energy comes out to be close to 100 atomic units, which is equal to the barrier height V_1 . From Fig. 5 it is clear that this choice of wave number leads to maximum rate. We also check the contribution due to the second term in Fig. 1 with k_1 interchanged with k_2 . For $k_1 = 600$, k_2 is close to 3000. For these two interchanged the amplitude is found to be four orders of magnitude smaller and hence negligible. We can, therefore, ignore the second amplitude for this choice of parameters.

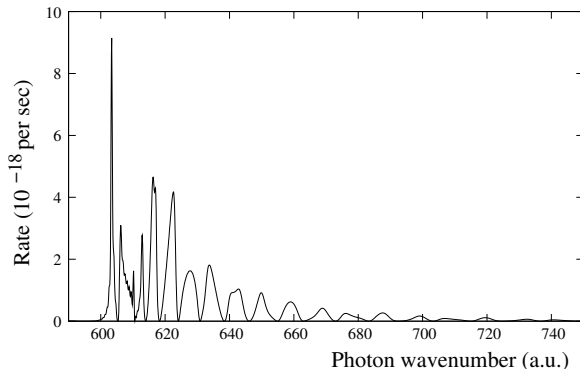


Figure 5: The reaction rate as a function of the wave of the photon emitted at the first vertex for $L_c = 10$. The rate shows very rapid fluctuations which are apparent in the figure.

As we increase the value of L_c we find that the dominant change occurs due to the normalization factors in the wave functions. Both the U_i and U_n wave functions contain a factor $\sqrt{L_c}$ in the denominator. Hence the rate shows an approximate decrease as $1/L_c^3$. In Fig. 6 we show the dependence of rate on L_c for $k_1 = 635$ atomic units for L_c up to 100. We have explicitly checked the dependence on L_c up to $L_c = 1000$ and the trend shown in Fig. 6 continues up to this value. At some sufficiently large value of L_c we expect a much sharper decrease, due to a delicate cancellation that was seen in the continuum case. However the numerical work to obtain this value of L_c becomes prohibitively time intensive and we do not pursue this in the current paper.

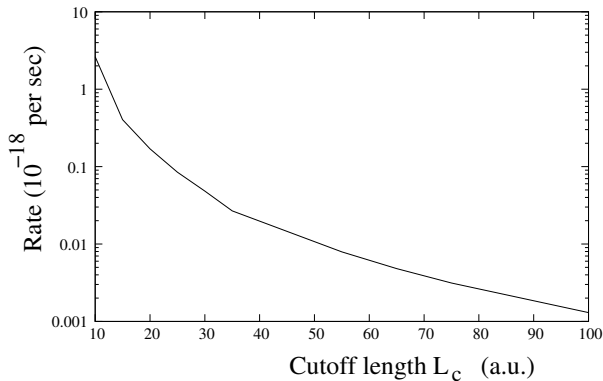


Figure 6: The reaction rate as a function of the cutoff length scale L_c for photon wave number $k_1 = 635$ atomic units. We find that the rate drops roughly as $1/L_c^3$.

5 Conclusions

We conclude that nuclear fusion reactions may be possible at low energies inside a medium through the mechanism of second order perturbation theory [12, 13, 14]. We find that the rate in free space turns out to be very small, in agreement with earlier results [12, 13]. The amplitude in

this case does become relatively large for intermediate state wave number values K_n close to the photon wave number k_1 . However as we sum over all intermediate wave numbers the amplitude becomes very small due to a delicate cancellation. In a medium, however, we expect that the energy eigenvalues would not be continuous. This is seen, for example, in a crystalline lattice which leads to a band structure with energy levels being separated by forbidden bands [15]. In a disordered system we expect to see localized states, analogous to Anderson localization [16, 17]. In either case we expect discontinuous energy eigenvalues. In the present paper we use a simple model by imposing a hard wall cutoff beyond a certain length scale. The essential feature of this model is that it leads to discretization of energy levels. This model leads to substantial rates for fusion reaction to take place at second order in perturbation theory. We obtain dominant contribution from intermediate states whose wave number K_n in the region $L_b < r < L_c$ is close to the photon wave number k_1 . The contribution is maximal if the intermediate states have energy close to the height of the potential barrier.

Our results suggest that, in favorable conditions, nuclear fusion reactions can take place at low energies at observable rates. However, so far we have only presented a toy model to test this phenomenon. Considerable more effort is needed to make contact with observations. This will require use of realistic models of the solid structure. Furthermore, photon emission may not be the dominant process and it would be interesting to consider other mechanisms.

References

- [1] Donald D. Clayton. *Principles of stellar evolution and nucleosynthesis*. The University of Chicago Press, Chicago, 1968.
- [2] Steven B. Krivit. *Development of Low-Energy Nuclear Reaction Research*, chapter 41, pages 479–496. John Wiley & Sons, Ltd, 2011.
- [3] Mahadeva Srinivasan, George Miley, and Edmund Storms. *Low-Energy Nuclear Reactions: Transmutations*, chapter 43, pages 503–539. John Wiley & Sons, Ltd, 2011.
- [4] Edmund Storms. Introduction to the main experimental findings of the lenr field. *Current Science*, 108:535–539, 02 2015.
- [5] Jean-Paul Biberian. Anomalous isotopic distribution of silver in a palladium cathode. *Journal of Condensed Matter Nuclear Science*, 29:211–218, 2019.
- [6] K. P. Sinha. Model of low energy nuclear reactions in a solid matrix with defects. *Current Science*, 108:516–518, 02 2015.
- [7] Francesco Celani, Antonino Tommaso, and Giorgio Vassallo. The zitterbewegung interpretation of quantum mechanics as theoretical framework for ultra-dense deuterium and low energy nuclear reactions. *Journal of Condensed Matter Nuclear Science*, 24:32–41, 02 2017.
- [8] C. Spitaleri, C.A. Bertulani, L. Fortunato, and A. Vitturi. The electron screening puzzle and nuclear clustering. *Physics Letters B*, 755:275 – 278, 2016.
- [9] Peter Hagelstein. Calculation of the boosted spin–orbit contribution to the phonon–nuclear coupling matrix element for ^{181}Ta . *Journal of Condensed Matter Nuclear Science*, 29:392–400, 02 2019.
- [10] Jean-Luc Paillet and Andrew Meulenberg. On highly relativistic deep electrons. *Journal of Condensed Matter Nuclear Science*, 29:472–492, 02 2019.

- [11] V. A. Chechin, V. A. Tsarev, M. Rabinowitz, and Y. E. Kim. Critical review of theoretical models for anomalous effects in deuterated metals. *International Journal of Theoretical Physics*, 33(3):617–670, Mar 1994.
- [12] P. Jain, A. Kumar, R. Pala, and K. P. Rajeev. Photon induced low-energy nuclear reactions. *Pramana*, 96(96), 2022.
- [13] P. Jain, A. Kumar, K. Ramkumar, R. Pala, and K. P. Rajeev. Low energy nuclear fusion with two photon emission. *JCMNS*, 35:1, 2021.
- [14] Péter Kálmán and Tamás Keszthelyi. Forbidden nuclear reactions. *Phys. Rev. C*, 99:054620, May 2019.
- [15] N. W. Ashcroft and N. D. Mermin. *Solid State Physics*. Holt-Saunders, 1976.
- [16] Elihu Abrahams. *50 Years of Anderson Localization*. WORLD SCIENTIFIC, 2010.
- [17] Patrick A. Lee and T. V. Ramakrishnan. Disordered electronic systems. *Rev. Mod. Phys.*, 57:287–337, Apr 1985.
- [18] E. Merzbacher. *Quantum Mechanics*. Wiley, 1998.
- [19] J.J. Sakurai. *Advanced Quantum Mechanics*. Always learning. Pearson Education, Incorporated, 1967.